DEUTSCHES ELEKTRONEN – SYNCHROTRON

DESY 92-049
MZ-TH/91-07
March 1992

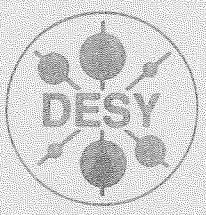

Exclusive Non-Leptonic Charm Baryon Decays

J. G. Körner, M. Krämer

Inst. für Physik, Johannes Gutenberg-Universität, Mainz

and

Deutsches Elektronen-Synchrotron DESY, Hamburg

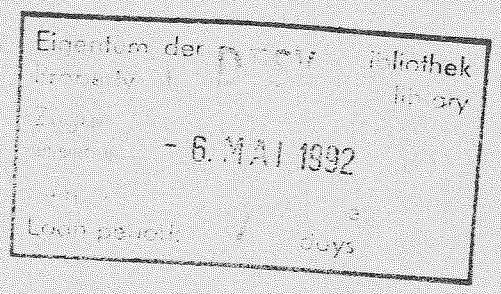

ISSN 0418-9833

NOTKESTRASSE 85 · D-2000 HAMBURG 52

ISSN 0418-9833

DESY 92-049
MZ-TH/91-07
March 1992

Exclusive Non-Leptonic Charm Baryon Decays

J.G. Körner*, M. Krämer*

Institut für Physik, Johannes Gutenberg-Universität,
Staudinger Weg 7, Postfach 3980
D-6500 Mainz, Germany

and

Deutsches Elektronen-Synchrotron DESY
Hamburg, Germany.

Abstract

We present a spectator quark model calculation of the Cabibbo-enhanced non-leptonic decays of the lowest lying charm baryons Λ_c, Ξ_c and Ω_c decaying into non-charm ground state baryons and mesons. We employ covariant quark model wave functions to describe the ground state baryons and mesons. They are obtained by boosting rest frame wave functions to equal velocity frames. The non-leptonic decay amplitudes are then obtained in terms of two wave function overlap parameters which we fit to the experimental data. We discuss general features of the flavour and helicity composition of the final states in the quark model approach. We emphasize that W-exchange contributions are of crucial importance for the description of non-leptonic charm baryon decay data. We calculate rates and polarization asymmetry parameters and compare them to existing data as well as to soft-meson plus current algebra calculations.

* Supported in part by the BMFT, FRG under contract 06MZ760

1 Introduction

In 1979 G. Kramer, J. Willrodt and one of us presented an exploratory quark model calculation of two-body and quasi-two-body non-leptonic (n.l.) charm baryon decays [1]. The paper was written before even any charm baryon decay had been identified let alone before mass and life time measurements of charm baryons existed.

The situation has dramatically changed in the intervening years. Many n.l. charm baryon decay modes have been observed in the meantime (see e.g. the review [2]). Among the observed two-body and quasi-two-body modes are $\Lambda_c^+ \to p\bar{K}^0$, $\Lambda_c^+ \to p\bar{K}^0(892)$, $\Lambda_c^+ \to \Delta^{++}K^-$, $\Lambda_c^+ \to \Lambda\pi^+$, $\Lambda_c^+ \to pf_0(975)$, $\Lambda_c^+ \to p\Phi$ [2], $\Lambda_c^+ \to \Sigma^0\pi^+$ [3,4], $\Xi_c^0 \to \Omega^-K^+$ and $\Xi_c^+ \to \Xi^-\pi^+$ [5]. Also the masses and lifetimes of the lowest lying charm baryon states are by now quite well known (see e.g. [2]). Furthermore, a wealth of new data on charm baryon decays is expected to become available in the next few years, in particular from the ARGUS and CLEO collaborations in e^+e^--collisions and from the hyperon beam experiments WA89 at CERN and E781 at Fermilab.

It is therefore timely to update and improve the quark model analysis of [1] incorporating the new experimental information on charm baryon masses, lifetimes and decay branching fractions. Also, recently there has been some improvement in the theoretical understanding of hadrons composed of heavy and light quarks and transitions among such heavy hadrons in the context of the Heavy Quark Effective Theory (HQET) [6] which puts the quark model approach to n.l. charm baryon decays on a much sounder theoretical footing. We also take the opportunity to correct some errors and misprints in [1]. We have added some material on angular decay distributions of the decay products in terms of joint angular decay distributions. Such an angular distribution analysis allows one to extract the dynamical information contained in experimental decay data.

2 Classification of states and their mass values

The ground state charm baryons are classified as usual as members of the (inequivalent) SU(4) multiplets 20′ and 20. The $J = 1/2$ ground state baryons (containing the ordinary $C = 0$ octet baryons) comprise the 20′ representation and the $J = 3/2$ ground state baryons (containing the ordinary $C = 0$ decuplet baryons) comprise the 20 representation. In Tables 1 and 2 we have listed the quantum number content and masses of the charm baryon members of the 20′ and 20 representation, where we now use the modern notation as recommended in [7].

There now exist precise mass measurements for the charm baryons Λ_c^+, Ξ_c^+, Ξ_c^0, Σ_c^{++}, Σ_c^+ and Σ_c^0 [2]. The remaining mass entries in Table 1 and 2 have been estimated in the framework of the one-gluon-exchange model of [8] (for details see [9]). In the non-relativistic Breit-Fermi reduction the one-gluon-exchange contribution leads to a spin-spin interaction of the form

$$H_{ss} = \sum_{i<j} \frac{16\pi\alpha_s}{9m_im_j} \vec{s}_i \cdot \vec{s}_j \delta^3(\vec{r}_i - \vec{r}_j) \quad . \tag{1}$$

Starting with the seminal work of [8] many authors have emphasized the fact that the hyperfine splitting resulting from (1) is crucial in understanding the mass breaking pattern of both

charm and charmless hadrons [10]. As long as the spin-spin interaction term is taken into account a variety of models with differing degrees of sophistication will basically reproduce the charm baryon mass pattern in Table 1 and 2. However, for our estimates of charm baryon masses in Table 1 and 2 we have retained the original version of the one-gluon-exchange model as detailed in [8].

Of the observed charm baryons, the Λ_c and the Ξ_c states are weakly decaying and thus their n.l. decay properties can be conveniently studied. According to the theoretical mass expectations, the unobserved Ω_c, Ξ_{cc}, Ω_{cc} and Ω_{ccc} states are anticipated to also be weakly decaying. However, in this paper we limit our attention to the lower mass $C=1$ baryons Λ_c^+, Ξ_c^+, Ξ_c^0 and Ω_c^0 leaving the discussion of the $C=2$ and $C=3$ baryons for future investigations.

A discussion of charm changing weak decays proceeds from the usual effective n.l. Hamiltonian [11]

$$H_{eff} = \frac{G_F}{\sqrt{2}} V_{cs} V_{ud}^* [c_- O_- + c_+ O_+] \tag{2}$$

where $O_\pm$ are local 4-quark operators

$$O_\pm = (\bar{u}_L \gamma_\mu d_L)(\bar{s}_L \gamma^\mu c_L) \pm (\bar{s}_L \gamma_\mu d_L)(\bar{u}_L \gamma^\mu c_L) \tag{3}$$

with $\bar{q}_L \gamma_\mu q_L = \frac{1}{2}\bar{q}\gamma_\mu(1-\gamma_5)q$, and $V_{q_\alpha q_\beta}$ are elements of the Kobayashi-Maskawa mixing matrix with $V_{cs} \simeq V_{ud} \simeq \cos\Theta_c$ and Θ_c the Cabibbo angle. The coefficients $c_\pm$ describe the leading log evolution of the n.l. Hamiltonian from the W-mass scale down to the charm mass scale $\mu \simeq O(m_c)$ [11]. For the QCD coefficients $c_\pm$ we take $c_+ = 0.73$ and $c_- = 1.90$ as in [1]; the value of the Kobayashi-Maskawa matrix element is $V_{cs} V_{ud}^* = (0.974)^2$ [7].

In the n.l. Hamiltonian (2) we have only written down the dominant contribution proportional to $\simeq \cos^2\Theta_c$. Once suppressed transitions proportional to $\simeq \cos\Theta_c \sin\Theta_c$ not written in (2) are the transition $c \to du\bar{d}$ and $c \to su\bar{s}$, and the doubly suppressed decay $c \to du\bar{s}$ proportional to $\simeq \sin^2\Theta_c$. In this paper we will mostly be concerned with the dominant $\cos^2\Theta_c$-piece of (2). The once and doubly suppressed n.l. charm baryon decays not discussed in this paper can be computed along the same lines once experimental information becomes available on these decays.

3 Quark model calculations

In the quark model the effective current×current Hamiltonian (2) gives rise to the five types of flavour diagrams drawn in Figure 1. We have chosen to label the quark lines for the specific transition $\Lambda_c^+ \to \Lambda\pi^+$ for illustrative purposes. The wavy lines are included in order to indicate how the effective quark currents of the Hamiltonian (2) act. As a next step, one wants to interprete the diagrams as Feynman diagrams possibly with additional gluon exchanges added. The general dynamical problem in all its complexity is far from being solved, so one has to resort to some approximation. The quark lines in Figure 1 transmit spin information from one hadron to the other. This is realized in the spectator quark model, which postulates that there is no spin communication between quark lines. Spin-spin interactions can be incorporated by introducing an effective spin-spin coupling between the two light quarks [12]. As the $\Sigma_c - \Lambda_c$ mass splitting shows they are not completely negligible. However, in this paper we limit ourselves to the spectator picture and neglect the spin-spin

interactions. Quark pairs are then created from the vacuum with $^3P_0$ quantum numbers which gives the model its name. Finally, these postulates can be cast into a covariant form if the quarks in a hadron are assumed to propagate with equal velocity which is also the hadron's velocity.

In terms of quark model spin wave functions, the decay amplitudes for the process $B_1 \to B_2 + M$ corresponding to Figure 1 can then be written as [1]

$$\begin{aligned} T_{B_1\to B_2+M} &= H_1 \bar{B}_2^{ABC'} B_{1ABC} \bar{M}_D^{D'} (O_{C'D'}^{CD} - \frac{1}{N_c} O_{D'C'}^{CD}) \\ &+ \frac{1}{N_c} H_2 \bar{B}_2^{AB'D} B_{1ABC} \bar{M}_D^{D'} O_{B'D'}^{BC} \\ &+ \frac{1}{N_c} H_2' \bar{B}_2^{AB'C'} B_{1ABC} \bar{M}_D^{B} O_{B'C'}^{CD} \\ &+ \frac{1}{N_c} H_3 \bar{B}_2^{A'B'C'} B_{1ABC} \bar{M}_{C'}^{C} O_{A'B'}^{AB} \end{aligned} \tag{4}$$

where the first, second, third and fourth terms of (4) correspond to the contributions of diagrams Ia,b, IIa, IIb and III in Figure 1 in that order. B_{ABC} and M_A^B are quark model wave functions for the baryons and mesons which will be specified later on. Each index A stands for a pair of indices (α, a), where α and a denote the spin and flavour degrees of freedom. We have already summed over colour degrees of freedom which results in the typical factors $1/N_c$ where $N_c = 3$. We emphasize that the limit $N_c \to \infty$ cannot be taken naively for the last three contributions in (4) (IIa,b and III in Figure 1). We shall return to this point later on. The matrix O_{AB}^{CD} describes the spin-flavour structure of the effective current×current Hamiltonian (2). H_1, H_2, H_2' and H_3 are wavefunction overlap integrals corresponding to diagrams I, IIa,b and III which are expected to depend on the masses of a particular decay process. Eq.(4) can be viewed as an algebraic realization of the diagrams shown in Figure 1: each line in Figure 1 corresponds to a contraction of doubly occurring spin-flavour indices in (4), where one sums over the spin-flavour indices.

The first term in (4) corresponds to the so-called factorization contribution and is calculated in terms of current matrix elements in Appendix A. Bringing the contributions of the non-factorizing diagrams IIa,b and III into tenable forms with the above assumptions does not preclude the possibility that (4) can be derived from a more general point of view dropping some of the above assumptions. One should note that in the case of transitions between ground state baryons, the non-factorizing diagrams IIa,b and III obtain contributions only from O^- (transforming as $20''$ in SU(4)) because of the symmetric nature of the ground state baryons [13]. Both operators O^+ and O^- contribute to diagram Ia and Ib. The contributions of Ia and Ib add up such that the resulting contribution is proportional to $\chi_\pm = (c_+(1+1/N_C) \pm c_-(1-1/N_C))/2$ depending on whether the final state meson is charged $(+)$ or neutral $(-)$.

The contribution of diagram Ib can be seen to be colour suppressed. Guided by the analysis of exclusive n.l. charm and bottom meson decays [14,15] we take the $N_c \to \infty$ limit and accordingly drop the contribution of diagram Ib in Figure 1 (cf. Appendix A). In the following we shall thus only include contributions from diagram Ia in Figure 1. Superficially also the contributions of diagrams IIa,b and III appear to be colour suppressed. But considering the fact that baryons contain N_c quarks as $N_c \to \infty$ the denominator factor N_c is balanced by combinatorial numerator expressions such that diagrams IIa,b and III occur at $\mathcal{O}(1)$ as

$N_c \to \infty$ and may not be dropped in this limit.

The results of calculating diagrams IIa,b and III will of course depend on the details of the quark model wave functions which are used as input. As in [1] we propose to use $SU(2)_W$ spin wave functions as a first approximation. They correspond to boosting static quark model wave functions to a collinear equal velocity frame as emphasized in [16]. The explicit forms of the wave functions are given by [17] (colour indices are always suppressed)

$$\begin{aligned} J^P = 1/2^+ &: \quad B_{ABC} = \frac{1}{M}\{[(\not{P} + M)\gamma_5 C]_{\beta\gamma} u_\alpha(P) B_{a[bc]} + \text{cycl.}(\alpha,a;\beta,b;\gamma,c)\} \\ J^P = 3/2^+ &: \quad B_{ABC} = \frac{1}{M}\{[(\not{P} + M)\gamma_\nu C]_{\beta\gamma} u_\alpha^\nu(P) B_{\{abc\}} + \text{cycl.}(\alpha,a;\beta,b;\gamma,c)\} \\ J^{PC} = 0^{-+} &: \quad M_A^B = [(\not{P} + M)\gamma_5]_\alpha^\beta M_a^b \\ J^{PC} = 1^{--} &: \quad M_A^B = [(\not{P} + M)\not{\epsilon}]_\alpha^\beta M_a^b \end{aligned} \tag{5}$$

for the hadrons in the initial state, and

$$\begin{aligned} J^P = 1/2^+ &: \quad \bar{B}_{ABC} = \frac{1}{M}\{[C^{-1}\gamma_5(\not{P} + M)]_{\beta\gamma} \bar{u}_\alpha(P) B_{a[bc]} + \text{cycl.}(\alpha,a;\beta,b;\gamma,c)\} \\ J^P = 3/2^+ &: \quad \bar{B}_{ABC} = \frac{1}{M}\{[C^{-1}\gamma_\nu(\not{P} + M)]_{\beta\gamma} \bar{u}_\alpha^\nu(P) B_{\{abc\}} + \text{cycl.}(\alpha,a;\beta,b;\gamma,c)\} \\ J^{PC} = 0^{-+} &: \quad \bar{M}_A^B = [(\not{P} - M)\gamma_5]_\alpha^\beta M_a^b \\ J^{PC} = 1^{--} &: \quad \bar{M}_A^B = [(\not{P} - M)\not{\epsilon}^*]_\alpha^\beta M_a^b \end{aligned} \tag{6}$$

for the hadrons in the final state. In (5) and (6) P and M denote the momentum and mass of the particles and C is the usual charge conjugation matrix. The $B_{a[bc]}$, $B_{\{abc\}}$ and M_a^b are baryonic and mesonic flavour wave functions. We have scaled out an explicit mass factor in the baryon wave functions to be in accord with the correct mass scaling factor in the heavy quark limit. The corresponding mass scaling factor in the meson case would be $1/\sqrt{M}$. However, as we are only dealing with pions and kaons in this paper, the unscaled meson wave functions in (5) and (6) are more appropriate.

With the explicit mass factors scaled out of the baryon wave functions one can then set $H_2 = H_2'$ in (4) due to CP-invariance [18]. After some straightforward algebraic manipulations involving the evaluation of the amplitude (4) with the covariant wave functions (5) and (6), one can calculate the n.l. transition amplitudes for the four decay classes $1/2^+ \to (1/2^+, 3/2^+) + (0^-, 1^-)$. We present our results in terms of invariant amplitudes defined in Appendix B where we denote the parity-violating (p.v.) and parity-conserving (p.c.) amplitudes by A and B, resp., in all four cases:

Case A : $1/2^+ \to 1/2^+ + 0^-$

$$\begin{aligned} A = A^{\text{fac}} &- \frac{H_2}{4M_1M_2} c_W c_- (M_1 P_1.P_2 - M_1 M_2^2 - M_1 M_2 M_3) 3 I_3 \\ &+ \frac{H_2}{4M_1M_2} c_W c_- (M_2 P_1.P_2 - M_1^2 M_2 - M_1 M_2 M_3) 3 \hat{I}_3 \\ B = B^{\text{fac}} &+ \frac{H_2}{4M_1M_2} c_W c_- M_1 Q_+ \frac{1}{2}(I_3 + 2I_4) \\ &+ \frac{H_2}{4M_1M_2} c_W c_- M_2 Q_+ \frac{1}{2}(\hat{I}_3 + 2\hat{I}_4) \\ &+ \frac{H_3}{4M_1M_2} c_W c_- M_1 M_2 (M_1 + M_2 + M_3) 12 I_5 \quad . \end{aligned} \tag{7}$$

The factorizing contributions A^{fac} and B^{fac} (corresponding to diagram Ia) are calculated in Appendix A. We have defined $Q_\pm = (M_1 \pm M_2)^2 - M_3^2$ and $c_W = \frac{G}{\sqrt{2}} V_{cs} V_{ud}^*$. The invariant flavour wave function contractions (Clebsch-Gordan coefficients) I_i and $\hat{I}_i$ appearing in (7) are defined in Appendix C (see also [1]). I_3 and I_4 are associated with diagram IIa, $\hat{I}_3$ and $\hat{I}_4$ with diagram IIb and I_5 with diagram III. Diagram III can be seen to contribute only to the p.c. amplitude B, whereas diagrams Ia and II contribute to both p.c. and p.v. amplitudes. The p.c. and p.v. amplitudes can be seen to be even and odd with respect to the generalized charge conjugation operation $(M_1; I_{3,4}; I_5) \to (M_2; \hat{I}_{3,4}; I_5)$ as expected from the CP-conserving property of the n.l. Hamiltonian. For example, for the decay $\Lambda_c^+ \to \Lambda\pi^+$ one finds $I_3 = \hat{I}_3$ and thus a vanishing of the p.v. amplitude A in the symmetry limit $M_1 = M_2$ as noted in [2]. With $M_1 \gg M_2$ one is far from the symmetry limit and one expects $A(\Lambda_c^+ \to \Lambda\pi^+) \neq 0$ in accord with recent experiments [19,4].

In order to establish contact to the current algebra approach to n.l. charm baryon decays note that there exist a one-to-one flavour correspondence with terms arising in the current algebra plus soft pion approach for the flavour structure in the p.v. amplitude A. This was first noticed empirically in the $\Delta C = 0$, $\Delta Y = 1$ [18] and in the $\Delta C = 0$, $\Delta Y = 0$ [20] transitions and was later proven in general [1]. The correspondence between the quark model and current algebra approach works in the following way: the contributions proportional to I_3 and $\hat{I}_3$ have the flavour struture of the "equal time commutator" term when the symmetry limit $M_1 = M_2$ is taken. The factorizing contribution A^{fac} has the same interpretation in both schemes. In a similar vein, the non-factorizing p.c. contributions to the amplitudes B can readily be interpreted as baryon pole contributions.

Case B : $1/2^+ \to 1/2^+ + 1^-$

In this case there are two p.v. and p.c. amplitudes each which are denoted as A_1, A_2 and B_1, B_2 (see Appendix B). One has

$$\begin{aligned} A_1 = A_1^{\text{fac}} &- \frac{H_2}{4M_1M_2} c_W c_- (M_1 P_1.P_2 - M_1 M_2^2 - M_1 M_2 M_3)(I_3 + 2I_4) \\ &- \frac{H_2}{4M_1M_2} c_W c_- (M_2 P_1.P_2 - M_1^2 M_2 - M_1 M_2 M_3)(\hat{I}_3 + 2\hat{I}_4) \\ A_2 = &- \frac{H_2}{4M_1M_2} c_W c_- (M_1^2 + M_1 M_2 + M_1 M_3)(I_3 + 2I_4) \\ &+ \frac{H_2}{4M_1M_2} c_W c_- (M_2^2 + M_1 M_2 + M_2 M_3)(\hat{I}_3 + 2\hat{I}_4) \\ B_1 = B_1^{\text{fac}} &+ \frac{H_2}{4M_1M_2} c_W c_- M_1 Q_+ \frac{1}{2}(I_3 + 2I_4) \\ &+ \frac{H_2}{4M_1M_2} c_W c_- M_2 Q_+ \frac{1}{2}(\hat{I}_3 + 2\hat{I}_4) \\ &+ \frac{H_3}{4M_1M_2} c_W c_- M_1 M_2 (M_1 + M_2 + M_3) 12 I_5 \\ B_2 = B_2^{\text{fac}} &- \frac{H_2}{4M_1M_2} c_W c_- \{(M_1^2 + M_1 M_2)(I_3 + 2I_4) - 3 M_1 M_3 I_3\} \\ &- \frac{H_2}{4M_1M_2} c_W c_- \{(M_2^2 + M_1 M_2)(\hat{I}_3 + 2\hat{I}_4) - 3 M_2 M_3 \hat{I}_3\} \\ &- \frac{H_3}{4M_1M_2} c_W c_- M_1 M_2 24 I_5 \quad . \end{aligned} \tag{8}$$

Again diagram III only contributes to the p.c. amplitudes B_i. Note that there is no factorizing contribution to the p.v. amplitude A_2. As in case A the contributions with the wrong C-parity vanish in the symmetry limit $M_1 = M_2$.

The decays involving $3/2^+$ states have a considerably simpler structure. First, note that the $3/2^+$ wave functions are separately symmetric in flavour and spin indices so that the contributions from diagrams IIb and III vanish as $\mathcal{H}^{20''}_{eff}$ is antisymmetric in flavour space [18]. In addition, a particular decay is contributed to by either diagram Ia or by diagram IIa but never by both. Thus the n.l. Λ_c^+- and Ξ_c^+-decays occur only via diagram IIa and the Ω_c^0-decays only via diagram Ia. This can again be seen by flavour symmetry arguments.

First we consider $1/2^+ \to 3/2^+ + 0^-$. One has

Case C : $1/2^+ \to 3/2^+ + 0^-$

$$\begin{aligned} A &= 0 \\ B &= B^{\rm fac} - \frac{H_2}{4M_1M_2} c_W c_- M_1 M_2 6 I_2^* \quad . \end{aligned} \tag{9}$$

Note that the p.v. amplitude in these decays is predicted to be zero [18]. Let us briefly pause to trace the sources of this important result. For the factorizing contribution our quark model ansatz leads to the familiar $M_{1+}(1/2^+ \to 3/2^+)$ conserved vector current transition which has no (pseudo)scalar component. A more general ansatz for the $1/2^+ \to 3/2^+$ transition form factor allowing for a spin-spin interaction between the two light quarks would feature a nonvanishing factorizing p.v. amplitude [21]. Clearly this prediction of our quark model needs experimental confirmation as e.g. in the n.l. decays $\Omega_c^0 \to \Xi^{*0}\bar{K}^0$ and $\Omega_c^0 \to \Omega^-\pi^+$. The absence of a p.v. transition from diagram IIa can again be understood by drawing the analogy to the current algebra+soft pion evaluation. In this approach the p.v. amplitude is predicted to be proportional to $f_\rho^{-1}\langle 3/2^+|\mathcal{H}_{p.c.}|1/2^+\rangle$ and this is zero in the quark model for the aforementioned reason [18]. The absence of a p.v. amplitude leads to a zero decay asymmetry. We mention that this quark model prediction [18] has been confirmed experimentally in the $s \to u$ sector for the decays $\Omega^- \to \Lambda K^-$, $\Omega^- \to \Xi^0\pi^-$ and $\Omega^- \to \Xi^-\pi^0$ [7].

As a last case we treat

Case D : $1/2^+ \to 3/2^+ + 1^-$

$$\begin{aligned} A_1 &= A_1^{\rm fac} - \frac{H_2}{4M_1M_2} c_W c_- (M_1 P_1.P_2 - M_1 M_2^2 - M_1 M_2 M_3) 6 I_2^* \\ A_2 &= 0 \\ A_3 &= A_3^{\rm fac} + \frac{H_2}{4M_1M_2} c_W c_- M_1 6 I_2^* \\ B_1 &= B_1^{\rm fac} - \frac{H_2}{4M_1M_2} c_W c_- M_1 Q_+ 3 I_2^* \\ B_2 &= B_2^{\rm fac} - \frac{H_2}{4M_1M_2} c_W c_- M_1 M_2 6 I_2^* \\ B_3 &= B_3^{\rm fac} + \frac{H_2}{4M_1M_2} c_W c_- M_1 6 I_2^* \quad . \end{aligned} \tag{10}$$

Before turning to our numerical results we discuss some more general features of the n.l. amplitudes (7-10).

One notes that the contributions of diagrams IIb and III in (7-10) are nonleading on the scale of the mass M_1 of the parent baryon. As a helicity analysis shows, they are nonleading

because the contributions IIb and III are suppressed by helicity as a result of the $(V-A)\times(V-A)$ nature of the underlying quark transition [22]. This implies that only the factorizing contribution Ia and the non-factorizing contribution IIa survive when $M_2/M_1 \to 0$. This conclusion holds in general for all the ground state decay channels cases A-D. These leading contributions can be seen to lead to an exclusive decay mode power behaviour $\Gamma \sim 1/M_1$ when M_2 and M_3 are kept fixed. The helicity suppressed contributions are down by an additional factor $(M_2/M_1)^2$. The same power behaviour holds true in n.l. meson decays. Compared to the inclusive n.l. rate $\Gamma^{nl}_{FQD} \sim M_1^5$ one infers that the exclusive branching ratio of a particular two-body channel decreases very rapidly as M_1 becomes large and M_2, M_3 are kept fixed. When both M_1 and M_2 become large with their ratios fixed, and M_3 kept fixed and small, one has again $\Gamma \sim (M_1)^5 \cdot (M_2/M_1)^6$ with the helicity suppressed contributions diagrams IIb, III down by another factor $(M_2/M_1)^2$. We do not, however, see a mechanism that would suppress the non-factorizing contribution IIa relative to the factorizing contribution in this limit as is implicit in the analysis of [23].

All these scaling laws can be explicitly checked by taking the appropriate limits in the power behaved form factor (12) in Section 4.

An interesting issue concerns the question whether the daughter baryon emerges from the decay process with positive or negative longitudinal polarization. The longitudinal polarization can easily be measured, in particular if the daughter baryon is self-analyzing in its decay as discussed in Appendix B. A quick appraisal of the quark model predictions with respect to this question is obtained by a leading M_1-power analysis of (7-10). The results of such an analysis are listed in Table 3 for the most interesting case $1/2^+ \to 1/2^+ + 0^-$. The weight of the contributions of diagrams IIa,b and III relative to the factorizing contribution Ia are determined by the unknown wave function overlap factors H_2 and H_3. A first experimental information on the longitudinal polarization of the daughter baryon exists for the decay $\Lambda_c^+ \to \Lambda\pi^+$ (see Section 4) with the result that the emerging Λ has a dominant negative longitudinal polarization, i.e. $H_{-\frac{1}{2}0} >> H_{\frac{1}{2}0}$. Table 3 shows that this is not unexpected as long as the contribution from diagram III is not dominant.

A similar analysis can easily be done for the decays $1/2^+ \to 1/2^+ + 1^-$ again analysing (8) w.r.t. the leading M_1 contributions.

4 Numerical results

The quark model amplitudes calculated in Section 3 contain a number of parameters (e.g. c_+, c_-, H_2, and H_3) which have to be estimated in order to be able to make any quantitative predictions about decay widths, branching ratios, asymmetry parameters etc. Since estimates of these parameters are at present afflicted with theoretical uncertainties, it is clear that those predictions of our quark model calculation must be considered most reliable which are independent of the particular values of the above parameters. A glance at (7-10) shows that the quark model amplitudes for the cases $1/2^+ \to 1/2^+ + 0^-(1^-)$ (7) and (8) are sufficiently complex that there are no parameter independent predictions which go beyond the I, U, and V sum rules written down in [1]. However, in the cases $1/2^+ \to 3/2^+ + 0^-(1^-)$ the quark model amplitudes are sufficiently simple so that the resulting structure is parameter independent to a considerable degree. Among these predictions are the zero asymmetry in the decays $1/2^+ \to 3/2^+ + 0^-$ and the vanishing of the decay modes $\Xi_c^+ \to \Sigma^{*+}\bar{K}^0(\bar{K}^{0*})$ and

$\Xi_c^+ \to \Xi^{*0}\pi^+(\rho^+)$.

Further results require the specification of the wave function overlap functions H_i and their dependence on the decay kinematics of a particular decay process. Intuitively one expects the overlap integrals to be largest in a zero recoil configuration, i.e. when the charm baryon at rest decays into non-charm baryon and meson pair at rest. As one is moving away from the zero recoil configuration and the decay products acquire momentum (or velocity) one must kick the initial quarks (or pair produced energetic quark-antiquark pairs in the final state) to catch up with the energetic quarks that come from the weak interaction vertex. Asymptotically such a picture results in power behaved suppression form factors, where the degree of the power fall-off depends on the number of quarks that need to be aligned to form the final state configuration. For the factorizing contribution Ia such a picture is realized by writing down a "dipole" type of form factor behaviour for the $B_1 \to B_2$ transition form factor in Ia. As the physics of the suppression of large recoil configurations is basically the same in all of the diagrams Ia, IIa,b and III we take this form factor effect into account by writing

$$H_i(M_1, M_2, M_3) = H_i \cdot F(M_1, M_2, M_3) \quad . \tag{11}$$

The H_i are mass independent zero recoil overlap parameters and $F(M_1, M_2, M_3)$ is a form factor function normalized to one at zero recoil. The form factor function is then parametrized as

$$F(M_1, M_2, M_3) = \left[\frac{1}{1 - M_3^2/m_{ff}^2} \cdot \left(1 - \frac{(M_1 - M_2)^2}{m_{ff}^2}\right)\right]^3 \tag{12Γ51}$$

where the power dependence (12) corresponds to taking an effective "dipole" behaviour for the form factor. Note that there is an intrinsic spin kinematic q^2-dependence in our quark model amplitudes which cancels one q^2-power of the form factor (12) to render it dipole-behaved. As an effective form factor mass for the non-factorizing diagrams IIa,b and III we take the mass of the $(\bar{c}s)$ vector meson state, i.e. we take $m_{ff} = m_{D_s^*} = 2.11$ GeV. For the factorizing diagrams we use nearest pole form factor masses as specified in Appendix A. As we are dealing with a wide range of pseudo-scalar and vector meson masses in our problem the form factor effect introduced through (12) is not negligible.

The zero recoil overlap parameters are then taken as free fit parameters except for the overlap of diagram Ia which we determine from factorization. Unfortunately there is no experimental information available on the zero recoil normalization of the $\Delta C = 1$ transition form factor. However, as a first approximation, we shall assume that the zero recoil normalization is one as would be the case in the heavy quark limit. A zero recoil normalization close to one is also featured by explicit quark model calculations [24]. The same unit normalization was used in the investigation of semi-leptonic $\Delta C = 1$ transitions in [25].

After having specified the zero recoil value of diagram Ia in Figure 1 one has only two free fit parameters, namely the zero recoil values of H_2 and H_3.

In Table 4 we list the experimental rate information on two-body decays of charm baryons. In addition to the rate measurement there exist two measurements of the asymmetry parameter in the decay $\Lambda_c^+ \to p\pi^+$ by the CLEO and ARGUS groups who quote $\alpha_c = -1.0 + 0.4$ [19] and $\alpha_c = -0.96 \pm 0.42$ [4], resp. For the absolute branching fraction of the reference decay $\Lambda_c^+ \to pK^-\pi^+$ we use two recent measurements by ARGUS [32] and CLEO [31], the mean value being $B_{\Lambda_c^+ \to pK^-\pi^+} = (4.3 \pm 1.4)\%$ [1]. Together with the lifetime of the Λ_c^+,

[1]We emphasize that the absolute two-body ratios used in our fit are subject to the uncertainties of the

$\tau_{\Lambda_c^+} = (2.0 \pm 0.18) \times 10^{-13}$ sec, one has

$$\Gamma(\Lambda_c^+ \to pK^-\pi^+) = 1.415 \times 10^{-13} \text{ GeV} \quad .$$

The accuracy of existing measurements is not good enough to allow for a precise analysis of the quark model predictions and an exact determination of the overlap parameters in terms of a systematic least square fit. In the following analysis we therefore do not include experimental errors considering the present calculation to be a first step towards a better understanding of the n.l. charm baryon decays. If more precise data become available one should repeat the fit including error estimates.

We adopt the following strategy to fit the values of the overlap integrals. We use the decays with the smallest experimental errors $\Lambda_c^+ \to p\bar{K}^0$ and $\Lambda_c^+ \to \Lambda\pi^+$ to determine H_2 and H_3, resp. $\Lambda_c^+ \to p\bar{K}^0$ has contributions from diagrams I and IIa and can therefore be used to fix the value of H_2. The weighted average of the listed measurements is $\Gamma(\Lambda_c^+ \to p\bar{K}^0)/\Gamma(\Lambda_c^+ \to pK^-\pi^+) = 0.49 \pm 0.07$. From this we find

$$H_2 = 0.119 \text{ GeV} \quad .$$

The value of H_3 can be extracted from the width of the decay $\Lambda_c^+ \to \Lambda\pi^+$, $\Gamma(\Lambda_c^+ \to \Lambda\pi^+)/\Gamma(\Lambda_c^+ \to pK^-\pi^+) = 0.17 \pm 0.04$, which is contributed to by all five decay diagrams. With the restriction that the asymmetry parameter in this decay is negative (which is true from the ARGUS and CLEO measurements with 99% C.L.) we can determine H_3 unambiguously to be

$$H_3 = -0.011 \text{ GeV} \quad .$$

The result of our fit indicates that the contribution of diagram III is strongly suppressed relative to diagrams I and IIa,b. We have no simple explanation for this suppression.

We are now in a position to make quantitative predictions for decay rates and angular distributions of all decays under consideration. The results of our calculation for the four different decay types (case A-D) are listed in Tables 5-8. As mentioned before there are quark model results which do not depend on the values of the various parameters used in the numerical calculation (cf. [1]). These are the vanishing of the asymmetry parameter in the decays $\Lambda_c^+ \to \Xi^0 K^+$ and $\Xi_c^+ \to \Sigma^+ K^-$ due to the vanishing of the p.v. amplitude B and the zero width of the decays $\Xi_c^+ \to \Sigma^{*+}\bar{K}^0(\bar{K}^{0*})$ and $\Xi_c^+ \to \Xi^{*0}\pi^+(\rho^+)$.

In Table 9 we compare our results to some of the current algebra calculations. The spread in the predictions indicates the model dependence of the results. In the next few years the advent of new data will certainly constrain the current algebra calculations further. The quark model fits the data quite well (at the cost of two parameters) except for the decays $\Lambda_c^+ \to p\bar{K}^0(892)$ and $\Lambda_c^+ \to \Delta^{++}K^-$ which come out too large compared to the present experimental values. All model calculations predict a negative asymmetry parameter value close to its maximum value -1 for the decay $\Lambda_c^+ \to \Lambda\pi^+$ and are thus in agreement with the measured asymmetry in this decay mode [19,4].

The decay modes $\Lambda_c^+ \to \Delta^{++}K^-$, $\Lambda_c^+ \to \Sigma^0\pi^+$ and $\Xi_c^0 \to \Omega^-K^+$ receive contributions only from the non-factorizing diagrams and thus give a measure of the non-factorizing contributions to the n.l. decays. Their rates indicate that the factorizing approximation to n.l.

branching ratio $B_{\Lambda_c^+ \to pK^-\pi^+}$. At present there exist four absolute measurements of $B_{\Lambda_c^+ \to pK^-\pi^+}$ which vary by a factor of two (see [33] and references therein).

charm baryon decays advocated in [23] may not always be a good approximation. In fact, the quark model results imply that factorizing and non-factorizing contributions enter with approximately equal weight, depending of course on the decay mode under consideration.

5 Conclusions

We have performed a quark model analysis of exclusive n.l. charm baryon decays. We have exhibited some general features of the factorizing ($\hat{=}$ "W-decay") and non-factorizing ($\hat{=}$ "W-exchange") quark model amplitudes using the simple spectator quark model picture where there is no spin communication between propagating quark lines. We then performed a numerical analysis by further specifying the values of two overlap parameters associated with the non-factorizing W-exchange contributions. These were obtained by a fit to available data. The results of our fit show that the W-exchange contributions are definitely needed to describe existing data on n.l. charm baryon decays.

The outcome of our fit shows that the overlap parameter H_3 associated with diagram III is much smaller than the overlap parameter H_2 associated with diagrams IIa,b. We have no direct physical interpretation of the strong suppression of the contribution of diagram III. It would be interesting to analyze the relative importance of diagrams IIa,b and III using explicit quark model wave functions.

An important simplifying feature of our spectator quark model approach is the assumption that there is no spin interaction between the light quarks while they are propagating between hadrons or while they are being created from the vacuum ("$^3P_0$"-model). This assumption leads to strong constraints on the helicity pattern of the charm baryon transitions which can be experimentally tested. Among these are the predictions of zero decay asymmetry in the decays $1/2^+ \to 3/2^+ + 0^-$. A future analysis of the decay structure of n.l. charm baryon decay data will show whether this simple spectator picture can be maintained or whether an additional effective spin-spin interaction between the light quarks is required [12].

Acknowledgement: We would like to acknowledge some informative discussions with B. Grinstein, T. Mannel and Z. Ryzak.

A Factorizing contributions

The contributions of the factorizing diagrams Ia and Ib in Figure 1 can be directly evaluated in terms of the current matrix elements:

$$T^{\rm fac}_{B_1\to B_2+M} = \frac{G}{\sqrt{2}} V_{cs}V^*_{ud}\chi_\pm \langle B_2|J^{V-A}_\mu|B_1\rangle\langle M|J^{\mu\,V-A}|0\rangle \quad . \tag{13}$$

The current matrix elements of the baryonic $1/2^+ \to 1/2^+$ and $1/2^+ \to 3/2^+$ transitions have been worked out in [21] using the covariant wave functions (5,6). In the approximation that there is no spin communication between the light quarks inside the baryon the transition can be described by just one form factor called $f(q^2)$ in the terminology of [21]. A second form factor called $g(q^2)$ in [21] can be introduced to describe possible spin-spin interactions of the light quarks. However, within the spirit of our spectator approach, we neglect this

contribution. The form factor $f(q^2)$ is normalized to one at maximum momentum transfer $q^2_{max} = (M_1 - M_2)^2$, $f(q^2_{max}) = 1$, according to the Heavy Quark Effective Theory.

We present our results for the factorizing diagram I in terms of invariant amplitudes defined in Appendix B :

Case A : $1/2^+ \to 1/2^+ + 0^-$

$$\begin{aligned} A^{\rm fac} &= \frac{1}{4M_1M_2} c_W\chi_\pm f_P Q_+(M_1 - M_2)(2I_1 + I_2)\cdot f(q^2) \\ B^{\rm fac} &= \frac{1}{4M_1M_2} c_W\chi_\pm f_P Q_+(M_1 + M_2)\frac{1}{3}(4I_1 + 5I_2)\cdot f(q^2) \end{aligned} \tag{14}$$

Case B : $1/2^+ \to 1/2^+ + 1^-$

$$\begin{aligned} A_1^{\rm fac} &= -\frac{1}{4M_1M_2} c_W\chi_\pm M_3^2 f_V Q_+\frac{1}{3}(4I_1 + 5I_2)\cdot f(q^2) \\ A_2^{\rm fac} &= 0 \\ B_1^{\rm fac} &= -A_1^{\rm fac} \\ B_2^{\rm fac} &= \frac{1}{4M_1M_2} c_W\chi_\pm M_3^2 f_V(M_1 + M_2)\frac{4}{3}(I_1 - I_2)\cdot f(q^2) \end{aligned} \tag{15}$$

Case C : $1/2^+ \to 3/2^+ + 0^-$

$$\begin{aligned} A^{\rm fac} &= 0 \\ B^{\rm fac} &= \frac{1}{4M_1M_2} c_W\chi_\pm f_P M_2(M_1 + M_2)4I_1^*\cdot f(q^2) \end{aligned} \tag{16}$$

Case D : $1/2^+ \to 3/2^+ + 1^-$

$$\begin{aligned} A_1^{\rm fac} &= \frac{1}{4M_1M_2} c_W\chi_\pm M_3^2 f_V Q_+ 2I_1^*\cdot f(q^2) \\ A_2^{\rm fac} &= 0 \\ A_3^{\rm fac} &= -\frac{1}{4M_1M_2} c_W\chi_\pm M_3^2 f_V 4I_1^*\cdot f(q^2) \\ B_1^{\rm fac} &= A_1^{\rm fac} \\ B_2^{\rm fac} &= \frac{1}{4M_1M_2} c_W\chi_\pm M_3^2 f_V M_2 4I_1^*\cdot f(q^2) \\ B_3^{\rm fac} &= A_3^{\rm fac} \quad , \end{aligned} \tag{17}$$

where $Q_\pm = (M_1 \pm M_2)^2 - M_3^2$, $c_W = \frac{G}{\sqrt{2}} V_{cs}V^*_{ud}$ and $\chi_\pm = (c_+(1 + 1/N_c) \pm c_-(1 - 1/N_c))/2$. The invariant flavour wave function contractions denoted as I_1, I_2, and I^* can be found in Appendix C.

The pseudoscalar meson coupling constants are defined by

$$\langle M^P(P_3)|A^\mu|0\rangle = f_P P_3^\mu \tag{18}$$

and the vector meson coupling constants by

$$\langle M^V(P_3)|V^\mu|0\rangle = M_3^2 f_V \bar{\epsilon}^\mu \quad . \tag{19}$$

For the meson decay constants we use the experimental values $f_\pi = 131.7$ MeV, $f_K = 160.6$ MeV and $f_\rho = 0.272$. For the vector meson decay constant we take the theoretical estimate of [39], $f_{K^*} = 0.238$.

The form factor $f(q^2)$ has to be continued from the normalization point $f(q^2_{max}) = 1$ to the momentum transfer of the respective decays $q^2 = (P_1 - P_2)^2 = P_3^2 = M_3^2$. The q^2-dependence of $f(q^2)$ is fixed by nearest meson dominance in the appropriate current channel. We take only two different form factor masses each for the $\bar{d}c$ and $\bar{s}c$ channels according to wether one has a vector current or axial vector current coupling. The q^2-dependence of the form factors is parametrized as in (12) with form factor masses

	$m_{ff}(1^-)$ [GeV]	$m_{ff}(1^+)$ [GeV]
$\bar{d}c$	2.01	2.42
$\bar{s}c$	2.11	2.54

The contributions of diagram I are proportional to the renormalization factor $\chi_\pm = \frac{1}{2}(c_+(1 + 1/N_c) \pm c_-(1 - 1/N_c))$. The value of $\chi_\pm$ depends crucially on the choice for the number of colours N_c. QCD implies $N_c = 3$ whereas phenomenological results in the decays of charmed mesons tend to favour $N_c \to \infty$ [14]. In the case of meson decays for $N_c \to \infty$ the matrix element factorizes and can be calculated in a simple manner [15]. We emphasize that this must not be true for baryonic transitions in general from colour counting alone and we therefore *assume* factorization for diagram I. The question of wether one should use $N_c = 3$ or $N_c \to \infty$ for the factorizing contribution diagram I can eventually be settled in a heuristic manner by analyzing the Cabibbo suppressed decay $\Lambda_c^+ \to p\Phi$ which is contributed to only by diagram I [2]. The amplitude of this decay mode contains no free parameters and is proportional to χ_-. For $N_c = 3$ we find for the total rate $\Gamma(\Lambda_c^+ \to p\Phi)/\Gamma(\Lambda_c^+ \to pK^-\pi^+) = 0.003$ and for $N_c \to \infty$ $\Gamma(\Lambda_c^+ \to p\Phi)/\Gamma(\Lambda_c^+ \to pK^-\pi^+) = 0.053$. Only the latter value is consistent with the experimentally observed number $(\Gamma(\Lambda_c^+ \to p\Phi)/\Gamma(\Lambda_c^+ \to pK^-\pi^+))_{\rm exp.} = 0.04 \pm 0.03$ (see Table 4). For the numerical evaluation of the decay amplitudes of diagram I we therefore take the limit $N_c \to \infty$, i.e. $\chi_\pm = \frac{1}{2}(c_+ \pm c_-)$.

B Amplitudes, rates and angular distributions

Definitions of invariant amplitudes and helicity amplitudes

In order to clearly differentiate parity-violating (p.v.) and parity-conserving (p.c.) amplitudes, the former will always be denoted by A_i and the latter by B_i. For convenience of notation, we introduce the abbreviations $Q_\pm = (M_1 \pm M_2)^2 - M_3^2$, where momenta and masses are labelled in the order $B(1) \to B(2) + M(3)$. The c.m. momenta of the decay products are then $p = \sqrt{Q_+Q_-}/(2M_1)$. We shall define parity-violating and parity-conserving helicity amplitudes for each case using

$$H^{\{{\rm p.c.}\atop{\rm p.v.}\}}_{-\lambda_2-\lambda_3} = \pm\eta_1\eta_2\eta_3(-1)^{s_1-s_2-s_3} H^{\{{\rm p.c.}\atop{\rm p.v.}\}}_{\lambda_2\lambda_3} \quad , \tag{20}$$

where η_i is the intrinsic parity and s_i the spin of particle i ($i = 1,2,3$) [40]. The upper (+) and lower (−) signs hold for the parity conserving and parity violating helicity amplitudes, respectively.

[2] The flavour couplings for this decay are given by $I_1 = I_2 = 1/\sqrt{6}$, $I_3 = I_4 = \hat{I}_3 = \hat{I}_4 = I_5 = 0$.

Case A : $1/2^+ \to 1/2^+ + 0^-$

Invariant amplitudes

$$\langle B_2M|\mathcal{H}_{eff}|B_1\rangle = \bar{u}(P_2)(A + B\gamma_5)u(P_1) \tag{21}$$

Helicity amplitudes

$$H^{\{{\rm p.v.}\atop{\rm p.c.}\}}_{\frac{1}{2}0} = H_{\frac{1}{2}0} \pm H_{-\frac{1}{2}0} = 2\left\{\begin{array}{c}\sqrt{Q_+}A\\ -\sqrt{Q_-}B\end{array}\right\} \tag{22}$$

Case B : $1/2^+ \to 1/2^+ + 1^-$

Invariant amplitudes

$$\langle B_2M|\mathcal{H}_{eff}|B_1\rangle = \bar{u}(P_2)\bar{\epsilon}_3^\beta(A_1\gamma_\beta\gamma_5 + A_2P_{1\beta}\gamma_5 + B_1\gamma_\beta + B_2P_{1\beta})u(P_1) \tag{23}$$

Helicity amplitudes

$$H^{\{{\rm p.v.}\atop{\rm p.c.}\}}_{\lambda_\alpha\lambda_\beta} = H_{\lambda_\alpha\lambda_\beta} \mp H_{-\lambda_\alpha-\lambda_\beta}$$

$$\begin{aligned} H^{\{{\rm p.v.}\atop{\rm p.c.}\}}_{-\frac{1}{2}-1} &= 2\sqrt{2}\left\{\begin{array}{c}\sqrt{Q_+}A_1\\ -\sqrt{Q_-}B_1\end{array}\right\} \\ H^{\{{\rm p.c.}\atop{\rm p.v.}\}}_{\frac{1}{2}0} &= \frac{2}{M_3}\left\{\begin{array}{l}\sqrt{Q_+}(M_1 - M_2)A_1 - \sqrt{Q_-}M_1pA_2\\ \sqrt{Q_-}(M_1 + M_2)B_1 + \sqrt{Q_+}M_1pB_2\end{array}\right\} \end{aligned} \tag{24}$$

Case C : $1/2^+ \to 3/2^+ + 0^-$

Invariant amplitudes

$$\langle B_2M|\mathcal{H}_{eff}|B_1\rangle = \bar{u}^\alpha(P_2)(AP_{1\alpha}\gamma_5 + BP_{1\alpha})u(P_1) \tag{25}$$

Helicity amplitudes

$$H^{\{{\rm p.v.}\atop{\rm p.c.}\}}_{\frac{1}{2}0} = H_{\frac{1}{2}0} \mp H_{-\frac{1}{2}0} = 2\sqrt{\frac{2}{3}}p\frac{M_1}{M_2}\left\{\begin{array}{c}-\sqrt{Q_-}A\\ \sqrt{Q_+}B\end{array}\right\} \tag{26}$$

Case D : $1/2^+ \to 3/2^+ + 1^-$

Invariant amplitudes

$$\begin{aligned} \langle B_2M|\mathcal{H}_{eff}|B_1\rangle &= \bar{u}^\alpha(P_2)\bar{\epsilon}_3^\beta(A_1g_{\alpha\beta} + A_2P_{1\alpha}\gamma_\beta + A_3P_{1\alpha}P_{1\beta} \\ &+ B_1g_{\alpha\beta}\gamma_5 + B_2P_{1\alpha}\gamma_\beta\gamma_5 + B_3P_{1\alpha}P_{1\beta}\gamma_5)u(P_1) \end{aligned} \tag{27}$$

Helicity amplitudes

$$H^{\{{\rm p.v.}\atop{\rm p.c.}\}}_{\lambda_\alpha\lambda_\beta} = H_{\lambda_\alpha\lambda_\beta} \pm H_{-\lambda_\alpha-\lambda_\beta}$$

$$H^{\{{\rm p.v.}\atop{\rm p.c.}\}}_{\frac{3}{2}\frac{1}{2}} = 2\left\{\begin{array}{c}-\sqrt{Q_+}A_1\\ \sqrt{Q_-}B_1\end{array}\right\}$$

$$H^{\{p.v.\}}_{-\frac{1}{2}-1} = \frac{2}{\sqrt{3}}\begin{Bmatrix} -\sqrt{Q_+}(A_1 - 2(Q_-/M_2)A_2) \\ \sqrt{Q_-}(B_1 - 2(Q_+/M_2)B_2) \end{Bmatrix}$$

$$H^{\{p.v.\}}_{\frac{1}{2}0} = \frac{2\sqrt{2}}{\sqrt{3}M_2M_3}\begin{Bmatrix} -\sqrt{Q_+}(\frac{1}{2}(M_1^2 - M_2^2 - M_3^2)A_1 \\ +Q_-(M_1+M_2)A_2 + M_1^2p^2A_3) \\ \sqrt{Q_-}(\frac{1}{2}(M_1^2 - M_2^2 - M_3^2)B_1 \\ -Q_+(M_1-M_2)B_2 + M_1^2p^2B_3) \end{Bmatrix} \quad . \tag{28}$$

Angular distribution and decay rates

Rates and angular decay distributions are given in terms of bilinear forms of the invariant amplitudes. Using standard methods [40,41] one can derive angular decay distributions, which, upon angle integration, give the decay rates. We prefer an explicit frame dependent representation of angular decay distributions instead of the frame independent representation discussed in [42]. First consider the (cascade) decay of an unpolarized charm baryon $1/2^+ \to 1/2^+(\to 1/2^+ + 0^-) + 0^-$ as for example in $\Lambda_c^+ \to \Lambda(\to p\pi^-) + \pi^+$. Referring to Figure 2 there is a cascade only on one side as the pion's decay goes unobserved. Consequently one has only a single polar angle distribution. One obtains

$$\frac{\mathrm{d}\Gamma(\Lambda_c^+ \to \Lambda(\to p\pi^-) + \pi^+)}{\mathrm{d}\cos\Theta_\Lambda} = \frac{1}{2}B_{\Lambda\to p\pi^-}\Gamma_{\Lambda_c^+\to\Lambda\pi^+}(1 + \alpha_c\alpha_\Lambda\cos\Theta_\Lambda) \quad . \tag{29}$$

α_c and α_Λ are the asymmetry parameters in the decays $\Lambda_c^+ \to \Lambda\pi^+$ and $\Lambda \to p\pi^-$, resp., defined by

$$\alpha_c = \frac{|H_{\frac{1}{2}0}|^2 - |H_{-\frac{1}{2}0}|^2}{|H_{\frac{1}{2}0}|^2 + |H_{-\frac{1}{2}0}|^2} \quad ; \quad \alpha_\Lambda = \frac{|h_{\frac{1}{2}0}|^2 - |h_{-\frac{1}{2}0}|^2}{|h_{\frac{1}{2}0}|^2 + |h_{-\frac{1}{2}0}|^2} \tag{30}$$

where $h_{\lambda_2\lambda_3}$ are the helicity amplitudes of the hyperon (cascade) decay defined in complete analogy to those of the charm baryon decays. The cascade decay $\Lambda \to p\pi^-$ acts as an analyzer of the longitudinal polarization of the daughter baryon Λ whose alignment polarization is given by the asymmetry parameter α_c. We mention that the angular decay distribution (29) was utilized experimentally in [19] and [4] to measure the asymmetry parameter α_c in the cascade decay $\Lambda_c^+ \to \Lambda(\to p\pi^-) + \pi^+$.

Somewhat more complicated is the three-fold decay distribution in the double cascade $1/2^+ \to 1/2^+(\to 1/2^+ + 0^-) + 1^-(\to 0^- + 0^-)$ as e.g. in $\Lambda_c^+ \to \Lambda(\to p\pi^-) + \rho^+(\to \pi^+\pi^0)$. One has

$$\frac{\mathrm{d}\Gamma(1/2^+ \to 1/2^+(\to 1/2^+ + 0^-) + 1^-(\to 0^- + 0^-)}{\mathrm{d}\cos\Theta\,\mathrm{d}\chi\,\mathrm{d}\cos\Theta_B} =$$

$$\frac{1}{2}\frac{1}{2\pi}B(B_2 \to B' + 0^-)B(M \to 0^- + 0^-)\frac{p}{32\pi M_1^2}$$

$$\Big[\frac{3}{4}\sin^2\Theta[|H_{\frac{1}{2}1}|^2(1 + \alpha_B\cos\Theta_B) + |H_{-\frac{1}{2}-1}|^2(1 - \alpha_B\cos\Theta_B)]$$

$$+\frac{3}{2}\cos^2\Theta[|H_{\frac{1}{2}0}|^2(1 + \alpha_B\cos\Theta_B) + |H_{-\frac{1}{2}0}|^2(1 - \alpha_B\cos\Theta_B)]$$

$$+\frac{3}{2\sqrt{2}}\alpha_B\cos\chi\sin\Theta_B\sin2\Theta\,\mathrm{Re}(H_{\frac{1}{2}1}H^*_{-\frac{1}{2}0} - H_{-\frac{1}{2}-1}H^*_{\frac{1}{2}0})\Big]$$

$$+\frac{3}{2\sqrt{2}}\alpha_B\sin\chi\sin\Theta_B\sin2\Theta\,\mathrm{Im}(H_{\frac{1}{2}1}H^*_{-\frac{1}{2}0} - H_{-\frac{1}{2}-1}H^*_{\frac{1}{2}0})\Big] \quad . \tag{31}$$

The polar angles Θ and Θ_B and the azimuthal angle χ are defined in Figure 3. The last term in (31) is proportional to the imaginary part of the longitudinal-transverse interference term. It is well known that the imaginary parts of interference terms contribute to a so-called T-odd observable. Such terms obtain contributions from CP-violating interactions and/or from effects of final-state interaction. The Standard Model CP-violating contributions are expected to be quite small and thus the imaginary part of the longitudinal-transverse interference term would be a good measure of the strength of final-state interaction effects. Alternatively, one may extract possible CP-violating effects by comparing Λ_c^+ and $\bar{\Lambda}_c^+$ cascade decays.

Double and single decay distributions as well as the rate may be obtained from (31) by the appropriate integrations. For the polar angle distribution of the cascade decay $1^- \to 0^+ + 0^+$ one has

$$\frac{\mathrm{d}\Gamma}{\mathrm{d}\cos\Theta} \propto 1 + \alpha_\Theta\cos^2\Theta \tag{32}$$

where

$$\alpha_\Theta = \frac{2|H_{\frac{1}{2}0}|^2 + 2|H_{-\frac{1}{2}0}|^2 - |H_{\frac{1}{2}1}|^2 - |H_{-\frac{1}{2}-1}|^2}{|H_{\frac{1}{2}1}|^2 + |H_{-\frac{1}{2}-1}|^2} \tag{33}$$

or, when expressed by the p.v. and p.c. helicity amplitudes,

$$\alpha_\Theta = 2\frac{|H^{p.c.}_{\frac{1}{2}0}|^2 + |H^{p.v.}_{\frac{1}{2}0}|^2}{|H^{p.c.}_{\frac{1}{2}1}|^2 + |H^{p.v.}_{\frac{1}{2}1}|^2} - 1 \quad . \tag{34}$$

A full discussion of all relevant angular decay distributions (including polarized charm baryon decays) can be found in [43].

The total rate, finally, is given by

$$\Gamma(B_1 \to B_2 + M) = \frac{p}{32\pi M_1^2}\sum_{hel.(\lambda_a - \lambda_\beta > 0)}\left(|H^{p.v.}_{\lambda_a\lambda_\beta}|^2 + |H^{p.c.}_{\lambda_a\lambda_\beta}|^2\right) \quad . \tag{35}$$

C Flavour space invariants

The transitions $1/2^+ \to 1/2^+ + 0^-(1^-)$ are represented by the seven SU(4) tensor invariants defined in (36)

$$\begin{aligned} I_1 &= \bar{B}^{a[bc]}B_{a[bc']}M^d_{d'}H^{[c'd']}_{[cd]} & I_2 &= \bar{B}^{a[bc]}B_{b[c'a]}M^d_{d'}H^{[c'd']}_{[cd]} \\ I_3 &= \bar{B}^{a[bc]}B_{a[b'c']}M^d_cH^{[c'b']}_{[db]} & I_4 &= \bar{B}^{b[ca]}B_{a[b'c']}M^d_cH^{[c'b']}_{[db]} \\ \hat{I}_3 &= \bar{B}^{a[bc]}B_{a[b'c']}M^{c'}_dH^{[db']}_{[cb]} & \hat{I}_4 &= \bar{B}^{a[bc]}B_{b'[c'a]}M^{c'}_dH^{[db']}_{[cb]} \\ I_5 &= \bar{B}^{a[bc]}B_{a'[b'c']}M^{c'}_cH^{[a'b']}_{[ab]} \end{aligned} \tag{36}$$

and the transitions $1/2^+ \to 3/2^+ + 0^-(1^-)$ by the two tensor invariants (37)

$$I_1^* = \bar{B}^{\{abc\}}B_{a[bc']}M^d_{d'}H^{[c'd']}_{[cd]} \qquad I_2^* = \bar{B}^{\{abc\}}B_{a[b'c']}M^d_cH^{[c'b']}_{[db]} \quad . \tag{37}$$

The flavour wave function contractions represent a convenient way of calculating the Clebsch-Gordon coefficients entering in n.l. charm baryon decays. They where first introduced in [1] which also contains some background material. Explicit representations of the flavour wave functions that are needed in this application can be found in [44]. For reasons of completeness the values of the invariants are given in Tables 10 and 11 for all decays under consideration.

References

[1] J.G. Körner, G. Kramer and J. Willrodt, *Z. Phys.* **C2**(1979)117

[2] J.G. Körner and H.W. Siebert, *Annu. Rev. Nucl. Part. Sci.* **41**(1991)511

[3] CLEO Collaboration (M. Procario, et al.), CMU-HEP-91-12 (1991)

[4] ARGUS Collaboration (H. Albrecht, et al.), *Phys. Lett.* **B274**(1992)239

[5] CLEO Collaboration (S. Henderson, et al.), CLNS-91-1125 (1991)

[6] N. Isgur and M.B. Wise, *Phys. Lett.* **237B**(1990)527;
J.D. Bjorken, in *Proc. Les Recontres de Physique de la Vallee de Aosta*, La Thuile, Italy. Gif-sur-Yvette: Ed. Frontieres(1990), p.583;
H. Georgi, *Phys. Lett.* **240B**(1990)447;
A.F. Falk, H. Georgi, B. Grinstein and M.B. Wise, *Nucl. Phys.* **B343**(1990)1;
B. Grinstein, *Nucl. Phys.* **B339**(1990)253;
E. Eichten and B. Hill, *Phys. Lett.* **234B**(1990)511;
F. Hussain, J.G. Körner, K. Schilcher, G. Thompson and Y.L. Wu, *Phys. Lett.* **249B**(1990)295

[7] Particle Data Group, *Phys. Lett.* **B239**(1990)

[8] A. De Rújula, H. Georgi and S.L. Glashow, *Phys. Rev.* **D12**(1975)147

[9] M. Krämer, in preparation

[10] W. Kwong, J.L. Rosner and C. Quigg, *Annu. Rev. Nucl. Part. Sci.* **37**(1987)325;
S. Capstick and N. Isgur, *Phys. Rev.* **D34**(1986)2809

[11] M.K. Gaillard and B.W. Lee, *Phys. Rev. Lett.* **33**(1974)108;
G. Altarelli and L. Maiani, *Phys. Lett.* **B52**(1974)351

[12] M. Krämer, diploma thesis, Mainz 1991

[13] J.G. Körner, *Nucl. Phys.* **B25**(1970)282;
J.G. Pati and C.H. Woo, *Phys. Rev.* **D3**(1971)2920

[14] M. Bauer and B. Stech, *Phys. Lett.* **B152**(1985)380

[15] A.J. Buras, J.M. Gérard and R. Rückl, *Nucl. Phys.* **B268**(1986)16

[16] F. Hussain, J.G. Körner and G. Thompson, *Ann. Phys.* **206**(1991)334

[17] R. Delbourgo, A. Salam and J. Strathdee, *Proc. Roy. Soc.* **A278**(1965)146;
T. Gudehus, DESY-68-11 (1968) (unpublished);
Phys. Rev. **184**(1969)1788

[18] J.G. Körner and T. Gudehus, *Nuovo Cim.* **11A**(1972)597

[19] CLEO Collaboration (P. Avery, et al.) *Phys. Rev. Lett.* **65**(1990)2842

[20] J.G. Körner, G. Kramer and J. Willrodt, *Phys. Lett.* **B81**(1979)365

[21] F. Hussain, J.G. Körner, M. Krämer and G. Thompson, *Z. Phys.* **C51**(1991)321;
F. Hussain, J.G. Körner, M.Krämer, D.S. Liu and S. Tawfiq, Trieste Preprint IC 91/133(1991) (to appear in Nucl. Phys. B)

[22] J.G. Körner and G.R. Goldstein, *Phys. Lett.* **B89**(1979)105

[23] J.D. Bjorken, *Phys. Rev.* **D40**(1989)1513;
T. Mannel, W. Roberts and Z. Ryzak, *Phys. Lett.* **B255**(1991)593;
A. Acker, S. Pakvasa, S.P. Rosen and S.F. Khan, *Phys. Rev.* **D43**(1991)3083

[24] M.B. Gavela, *Phys. Lett.* **B83**(1979)367;
R. Pérez-Marcial et al., *Phys. Rev.* **D40**(1989)2955;
R. Singleton, *Phys. Rev.* **D43**(1991)2939

[25] F. Hussain and J.G. Körner, *Z. Phys.* **C51**(1991)607

[26] J.M. Weiss in *Proc. Baryon 1980 Conf.*, Toronto, July 14-16, 1980, p.319 (1980)

[27] M.Basile, et al., *Nuovo Cim.* **62A**(1981)14

[28] ARGUS Collaboration (H. Albrecht, et al.), *Phys. Lett.* **207B**(1988)109

[29] S. Barlag, et al. *Z. Phys.* **C48**(1990)29

[30] J.C. Anjos, et al., *Phys. Rev.* **D41**(1990)801

[31] CLEO Collaboration (P. Avery, et al.) *Phys. Rev.* **D43**(1991)3599

[32] ARGUS Collaboration (H. Albrecht, et al.), *Phys. Lett.* **B210**(1988)263

[33] CLEO Collaboration (P. Avery, et al.), Contribution to the EP-HEP Conference, Geneva (1991)

[34] F. Hussain and K. Khan, *Nuovo Cim.* **88A**(1985)213;
F. Hussain and M. Scadron, *Nuovo Cim.* **79A**(1984)248

[35] H.Y. Cheng and B. Tseng, IP-ASTP-17-91 (1991)

[36] D. Ebert and W. Kallies, *Z. Phys.* **C29**(1985)643

[37] S. Pakvasa, S. Tuan and S.P. Rosen, *Phys. Rev.* **D42**(1990)3746

[38] Q.P. Xu and A.N. Kamal, Alberta THY-8-92 (1992)

[39] L.J. Reinders, H. Rubinstein and S. Yazaki, *Phys. Rep.* **127**(1985)1

[40] J.D. Jackson in *High Energy Physics*, ed. C. de Witt and R. Gatto. New York, Gordon and Breach (1965), p. 325

[41] A.D. Martin and D. Spearman, *Elementary Particle Theory.* Amsterdam, North-Holland (1970);
R. Pilkuhn, *The Interactions of Hadrons.* Amsterdam, North-Holland (1967)

[42] J.D. Bjorken, *Phys. Rev.* **D40**(1989)1513

[43] J.G. Körner, M.Krämer and K. Zalewski, Mainz Preprint, MZ-TH/91-06 (1991)

[44] J.G. Körner, *Z. Phys.* **C33**(1987)529

Figure Captions

Figure 1 Quark diagrams contributing to n.l. decay $\Lambda_c^+ \to \Lambda\pi^+$ including colour-flavour weight factors.

Figure 2 Definition of polar angle Θ_Λ in the decay $\Lambda_c^+ \to \Lambda(\to p\pi^-) + \pi^+$.

Figure 3 Definition of polar angles $\Theta_\Lambda = \Theta_B$ and Θ and azimuthal angle χ in the double cascade decay $\Lambda_c^+ \to \Lambda(\to p\pi^-) + \rho^+(\to \pi^+\pi^0)$.

Table 1. Charmed $1/2^+$ baryon states. $[ab]$ and $\{ab\}$ denote antisymmetric and symmetric flavour index combinations. Exp. masses for Λ_c, Ξ_c and Σ_c from [2]. Other mass values are theoretical estimates taken from [9]

Notation	Quark content	SU(3)	(I, I_3)	S	C	Mass
Λ_c^+	$c[ud]$	3^*	(0, 0)	0	1	2285.0 ± 0.6 MeV
Ξ_c^+	$c[su]$	3^*	(1/2, 1/2)	-1	1	2466.2 ± 2.2 MeV
Ξ_c^0	$c[sd]$	3^*	(1/2, -1/2)	-1	1	2472.8 ± 1.7 MeV
Σ_c^{++}	cuu	6	(1, 1)	0	1	2453 ± 0.9 MeV
Σ_c^+	$c\{ud\}$	6	(1, 0)	0	1	2453 ± 3.6 MeV
Σ_c^0	cdd	6	(1, -1)	0	1	2452.5 ± 0.9 MeV
$\Xi_c^{+\prime}$	$c\{su\}$	6	(1/2, 1/2)	-1	1	2.57 GeV
Ξ_c^0	$c\{sd\}$	6	(1/2, -1/2)	-1	1	2.57 GeV
Ω_c^0	css	6	(0, 0)	-2	1	2.69 GeV
Ξ_{cc}^{++}	ccu	3	(1/2, 1/2)	0	2	3.61 GeV
Ξ_{cc}^+	ccd	3	(1/2, -1/2)	0	2	3.61 GeV
Ω_{cc}^+	ccs	3	(0, 0)	-1	2	3.71 GeV

Table 2. Charmed $3/2^+$ baryon states. Theoretical mass estimates from [9]

Notation	Quark content	SU(3)	(I, I_3)	S	C	Mass (GeV)
Σ_c^{*++}	cuu	6	(1, 1)	0	1	2.51
Σ_c^{*+}	cud	6	(1, 0)	0	1	2.51
Σ_c^{*0}	cdd	6	(1, -1)	0	1	2.51
Ξ^{*+}	cus	6	(1/2, 1/2)	-1	1	2.63
Ξ^{*0}	cds	6	(1/2, -1/2)	-1	1	2.63
Ω_c^{*0}	css	6	(0, 0)	-2	1	2.74
Ξ_{cc}^{*++}	ccu	3	(1/2, 1/2)	0	2	3.68
Ξ_{cc}^{*+}	ccd	3	(1/2, -1/2)	0	2	3.68
Ω_{cc}^{*+}	ccs	3	(0, 0)	-1	2	3.76
Ω_{ccc}^{++}	ccc	1	(0, 0)	0	3	4.73

Table 3. Leading helicity coefficients for charmed baryon decays. Coefficients are calculated from the SU(4) invariants I_i and $\hat{I}_i$ as defined in [1] (see also Appendix C). η_1 and η_8 are SU(3) singlet and octet states as in [1]. The relative normalization of different diagrams is given by the leading M_1-coefficient of the explicit quark model expressions (7-10). Contributions from diagrams IIb and III are chirality suppressed ($\times$)

	$H^{Ia}_{\frac{1}{2}0}$	$H^{Ia}_{\frac{3}{2}0}$	$H^{Ib}_{\frac{3}{2}0}$	$H^{Ia}_{\frac{1}{2}0}$	$H^{Ib\times}_{\frac{1}{2}0}$	$H^{Ib\times}_{\frac{3}{2}0}$	$H^{III\times}_{\frac{1}{2}0}$	$H^{III\times}_{\frac{3}{2}0}$
	$5I_1 + 4I_2$	$I_1 - I_2$	$-\frac{3}{2}(I_3 - I_4)$	$-\frac{3}{2}(2I_3 + I_4)$	$-\frac{3}{2}(\hat{I}_3 - \hat{I}_4)$	$-\frac{3}{2}(2\hat{I}_3 + \hat{I}_4)$	$18I_5$	$-18I_5$
$6\Lambda_c^+ \to \Lambda\pi^+$	−18	0	9	0	9	0	18	−18
$\sqrt{12}\Lambda_c^+ \to \Sigma^0\pi^+$	0	0	3	6	−9	0	−18	18
$\sqrt{12}\Lambda_c^+ \to \Sigma^+\pi^0$	0	0	−3	−6	9	0	18	−18
$6\Lambda_c^+ \to \Sigma^+\eta_8$	0	0	9	0	−9	0	18	−18
$\sqrt{18}\Lambda_c^+ \to \Sigma^+\eta_1$	0	0	−9	−9	−9	0	18	−18
$\sqrt{18}\Lambda_c^+ \to p\bar{K}^0$	−9	0	6	3	0	0	0	0
$\sqrt{6}\,\Lambda_c^+ \to \Xi^0 K^+$	0	0	3	−3	0	0	18	−18
$\sqrt{6}\,\Xi_c^+ \to \Sigma^+\bar{K}^0$	−9	0	0	0	9	0	0	0
$\sqrt{6}\,\Xi_c^+ \to \Xi^0\pi^+$	9	0	0	0	−9	0	0	0
$6\,\Xi_c^0 \to \Lambda\bar{K}^0$	9	0	−9	−9	9	0	18	−18
$\sqrt{12}\,\Xi_c^0 \to \Sigma^0\bar{K}^0$	9	0	−3	3	−9	0	−18	18
$\sqrt{6}\,\Xi_c^0 \to \Sigma^+ K^-$	0	0	3	−3	0	0	18	−18
$\sqrt{12}\,\Xi_c^0 \to \Xi^0\pi^0$	0	0	−6	−3	9	0	0	0
$6\,\Xi_c^0 \to \Xi^0\eta_8$	0	0	0	9	−9	0	−36	36
$\sqrt{18}\,\Xi_c^0 \to \Xi^0\eta_1$	0	0	−9	−9	−9	0	18	−18
$\sqrt{6}\,\Xi_c^0 \to \Xi^-\pi^+$	−9	0	6	3	0	0	0	0
$\Omega_c^0 \to \Xi^0\bar{K}^0$	1	2	0	0	−3	−6	0	0
$\Lambda_c^+ \to \Lambda K^+$	−18	0	0	9	−9	0	36	−36
$\sqrt{6}\,\Lambda_c^+ \to \Sigma^+ K^0$	0	0	0	9	9	0	0	0

Table 4. Measured Λ_c^+ branching ratios relative to $\Lambda_c^+ \to pK^-\pi^+$

	Mark II [26]	R415 [27]	ARGUS [4,28]	NA 32 [29]	E691 [30]	CLEO [3,5,31]
$p\bar{K}^0$	$.50 \pm .25$		$.62 \pm .15$		$.55 \pm .22$	$.44 \pm .09$
$p\bar{K}^0(892)$	$.18 \pm .10$	$.42 \pm .24$				
$\Delta^{++}K^-$	$.17 \pm .07$	$.40 \pm .17$				
$\Lambda\pi^+$			$.18 \pm .05$			$.17 \pm .04$
$\Sigma^0\pi^+$			$.15 \pm .08$			$.17 \pm .06$
$p\Phi$				$.04 \pm .03$		
$\frac{\Xi_c^0 \to \Omega^- K^+}{\Xi_c^0 \to \Xi^-\pi^+}$						$.50 \pm .21$

Table 5. Partial widths and asymmetry α_c for decays $1/2^+ \to 1/2^+ 0^-$. For definition of charm baryon asymmetry parameter α_c see (30)

	$\Gamma[10^{11}\,s^{-1}]$	α_c		$\Gamma\,[10^{11}\,s^{-1}]$	α_c
$\Lambda_c^+ \to \Lambda\pi^+$	0.37	−0.70	$\Xi_c^0 \to \Lambda\bar{K}^0$	0.11	−0.76
$\Lambda_c^+ \to \Sigma^0\pi^+$	0.16	+0.70	$\Xi_c^0 \to \Sigma^0\bar{K}^0$	1.05	−0.96
$\Lambda_c^+ \to \Sigma^+\pi^0$	0.16	+0.71	$\Xi_c^0 \to \Sigma^+ K^-$	0.11	0
$\Lambda_c^+ \to \Sigma^+\eta$	0.08	+0.33	$\Xi_c^0 \to \Xi^0\pi^0$	0.03	+0.92
$\Lambda_c^+ \to \Sigma^+\eta'$	0.64	−0.45	$\Xi_c^0 \to \Xi^0\eta$	0.21	−0.92
$\Lambda_c^+ \to p\bar{K}^0$	1.05	−1.0	$\Xi_c^0 \to \Xi^0\eta'$	0.76	−0.38
$\Lambda_c^+ \to \Xi^0 K^+$	0.13	0	$\Xi_c^0 \to \Xi^-\pi^+$	0.93	−0.38
$\Xi_c^+ \to \Sigma^+\bar{K}^0$	1.46	−1.0	$\Omega_c^0 \to \Xi^0\bar{K}^0$	1.75	+0.51
$\Xi_c^+ \to \Xi^0\pi^+$	0.80	−0.78			

Table 6. Partial widths and asymmetry α_Θ for decays $1/2^+ \to 1/2^+ + 1^-$. For definition of asymmetry parameter α_Θ see (33)

	$\Gamma[10^{11}\,s^{-1}]$	α_Θ		$\Gamma\,[10^{11}\,s^{-1}]$	α_Θ
$\Lambda_c^+ \to \Lambda\rho^+$	9.54	+3.02	$\Xi_c^0 \to \Lambda\bar{K}^{*0}$	1.00	+0.58
$\Lambda_c^+ \to \Sigma^0\rho^+$	1.57	+0.29	$\Xi_c^0 \to \Sigma^0\bar{K}^{*0}$	0.55	−0.87
$\Lambda_c^+ \to \Sigma^+\rho^0$	1.56	+0.30	$\Xi_c^0 \to \Sigma^+K^{*-}$	0.35	−0.60
$\Lambda_c^+ \to \Sigma^+\omega$	2.01	+0.19	$\Xi_c^0 \to \Xi^0\rho^0$	1.53	−0.33
$\Lambda_c^+ \to \Sigma^+\Phi$	0.13	+7.50	$\Xi_c^0 \to \Xi^0\omega$	2.08	+1.09
$\Lambda_c^+ \to p\bar{K}^{*0}$	1.54	−0.02	$\Xi_c^0 \to \Xi^0\Phi$	0.16	+17.67
$\Lambda_c^+ \to \Xi^0K^{*+}$	0.06	−0.76	$\Xi_c^0 \to \Xi^-\rho^+$	10.97	+4.36
$\Xi_c^+ \to \Sigma^+\bar{K}^{*0}$	0.53	−0.90	$\Omega_c^0 \to \Xi^0\bar{K}^{*0}$	0.85	−0.01
$\Xi_c^+ \to \Xi^0\rho^+$	21.68	+1.13			

Table 7. Partial widths for decays $1/2^+ \to 3/2^+ + 0^-$. A cross (×) denotes kinematically forbidden processes

	$\Gamma[10^{11}\,s^{-1}]$		$\Gamma\,[10^{11}\,s^{-1}]$
$\Lambda_c^+ \to \Sigma^{*0}\pi^+$	0.25	$\Xi_c^0 \to \Sigma^{*0}\bar{K}^0$	0.22
$\Lambda_c^+ \to \Sigma^{*+}\pi^0$	0.25	$\Xi_c^0 \to \Sigma^{*+}\bar{K}^-$	0.44
$\Lambda_c^+ \to \Sigma^{*+}\eta$	0.52	$\Xi_c^0 \to \Xi^{*0}\pi^0$	0.25
$\Lambda_c^+ \to \Sigma^{*+}\eta'$	×	$\Xi_c^0 \to \Xi^{*0}\eta$	0.02
$\Lambda_c^+ \to \Delta^+\bar{K}^0$	0.45	$\Xi_c^0 \to \Xi^{*0}\eta'$	×
$\Lambda_c^+ \to \Delta^{++}K^-$	1.35	$\Xi_c^0 \to \Xi^{*-}\pi^+$	0.50
$\Lambda_c^+ \to \Xi^{*0}K^+$	0.25	$\Xi_c^0 \to \Omega^-K^+$	0.30
$\Xi_c^+ \to \Sigma^{*+}\bar{K}^0$	0	$\Omega_c^0 \to \Xi^{*0}\bar{K}^0$	0.20
$\Xi_c^+ \to \Xi^{*0}\pi^+$	0	$\Omega_c^0 \to \Omega^-\pi^+$	0.86

Table 8. Partial widths for decays $1/2^+ \to 3/2^+ + 1^-$. A cross (×) denotes kinematically forbidden processes

	$\Gamma[10^{11}\,s^{-1}]$		$\Gamma\,[10^{11}\,s^{-1}]$
$\Lambda_c^+ \to \Sigma^{*0}\rho^+$	0.58	$\Xi_c^0 \to \Sigma^{*0}\bar{K}^{*0}$	0.97
$\Lambda_c^+ \to \Sigma^{*+}\rho^0$	0.58	$\Xi_c^0 \to \Sigma^{*+}\bar{K}^{*-}$	2.00
$\Lambda_c^+ \to \Sigma^{*+}\omega$	0.51	$\Xi_c^0 \to \Xi^{*0}\rho^0$	0.82
$\Lambda_c^+ \to \Sigma^{*+}\Phi$	×	$\Xi_c^0 \to \Xi^{*0}\omega$	0.75
$\Lambda_c^+ \to \Delta^+\bar{K}^{*0}$	1.50	$\Xi_c^0 \to \Xi^{*0}\Phi$	×
$\Lambda_c^+ \to \Delta^{++}K^{*-}$	4.78	$\Xi_c^0 \to \Xi^{*-}\rho^+$	1.60
$\Lambda_c^+ \to \Xi^{*0}K^{*+}$	×	$\Xi_c^0 \to \Omega^-K^{*+}$	×
$\Xi_c^+ \to \Sigma^{*+}\bar{K}^{*0}$	0	$\Omega_c^0 \to \Xi^{*0}\bar{K}^{*0}$	1.13
$\Xi_c^+ \to \Xi^{*0}\rho^+$	0	$\Omega_c^0 \to \Omega^-\rho^+$	5.07

Table 9. Current algebra and quark model predictions for n.l. Λ_c^+ decays. The numbers cited are branching rates (relative to $\Lambda_c^+ \to pK^-\pi^+$) and asymmetry parameters α_c

	HK [34]	CT [35]	EK [36]	PTR [37]	XK [38]	Quark model
$\Lambda_c^+ \to p\bar{K}^0$	0.16	0.28	0.08	1.3	0.28	input
(α_c)	(−0.77)	(−0.49)	(−0.82)	(−0.61)	(+0.51)	(−1.0)
$\Lambda_c^+ \to \Lambda\pi^+$	0.35	0.20	0.15	0.5	0.38	input
(α_c)	(−0.89)	(−0.96)	(−1.0)	(−1.0)	(−0.67)	(−0.70)
$\Lambda_c^+ \to p\bar{K}^0(892)$		0.42		0.13		0.72
$\Lambda_c^+ \to p\Phi$		0.05				0.05
$\Lambda_c^+ \to \Delta^{++}K^-$						0.63
$\Lambda_c^+ \to \Sigma^0\pi^+$	1.03	0.17	0.10		0.08	0.08
$\frac{\Xi_c^0 \to \Omega^-K^+}{\Xi_c^0 \to \Xi^-\pi^+}$						0.32

Table 10. Values for SU(4) invariants for ground state $1/2^+$ baryons. Various identities for these invariants can be found in [1]. The η_8 appearing in the table is the unphysical $I = 0$, $Y = 0$ SU(3) octet state. We have also included values of the tensor invariants for the unphysical SU(3) singlet state η_1. The corresponding values for the physical states η and η' are obtained from the linear combinations $\sqrt{6}\,\eta = (1+\sqrt{2})\eta_8 - (1-\sqrt{2})\eta_1$ and $\sqrt{6}\,\eta' = (1-\sqrt{2})\eta_8 + (1+\sqrt{2})\eta_1$. Similarly the appropriate combinations for the physical states ω and ϕ (using ideal mixing) are $\phi = -\sqrt{2/3}\,\eta_8 + \sqrt{1/3}\,\eta_1$ and $\omega = \sqrt{1/3}\,\eta_8 + \sqrt{2/3}\,\eta_1$. We have always factored out the product of flavour space quark model wave function normalizations

	I_1	I_2	I_3	I_4	$\hat{I}_3$	$\hat{I}_4$	I_5
$6\,\Lambda_c^0 \to \Lambda\pi^+$	−2	−2	−2	4	−2	4	1
$\sqrt{12}\,\Lambda_c^+ \to \Sigma^0\pi^+$	0	0	−2	0	2	−4	−1
$\sqrt{12}\,\Lambda_c^+ \to \Sigma^+\pi^0$	0	0	2	0	−2	4	1
$6\,\Lambda_c^3 \to \Sigma^+\eta_8$	0	0	−2	4	2	−4	1
$\sqrt{18}\,\Lambda_c^+ \to \Sigma^+\eta_1$	0	0	4	−2	2	−4	1
$\sqrt{6}\,\Lambda_c^+ \to p\bar{K}^0$	−1	−1	−2	2	0	0	0
$\sqrt{6}\,\Lambda_c^+ \to \Xi^0K^+$	0	0	0	2	0	0	1
$\sqrt{6}\,\Xi_c^+ \to \Sigma^+\bar{K}^0$	−1	−1	0	0	−2	4	0
$\sqrt{6}\,\Xi_c^+ \to \Xi^0\pi^+$	1	1	0	0	2	−4	0
$6\,\Xi_c^0 \to \Lambda\bar{K}^0$	1	1	4	−2	−2	4	1
$\sqrt{12}\,\Xi_c^0 \to \Sigma^0\bar{K}^0$	1	1	0	−2	2	−4	−1
$\sqrt{6}\,\Xi_c^0 \to \Sigma^+K^-$	0	0	0	2	0	0	1
$\sqrt{12}\,\Xi_c^0 \to \Xi^0\pi^0$	0	0	2	−2	−2	4	0
$6\,\Xi_c^0 \to \Xi^0\eta_8$	0	0	−2	−2	2	−4	−2
$\sqrt{18}\,\Xi_c^0 \to \Xi^0\eta_1$	0	0	4	−2	2	−4	1
$\sqrt{6}\,\Xi_c^0 \to \Xi^-\pi^+$	−1	−1	−2	2	0	0	0
$\Omega_c^0 \to \Xi^0\bar{K}^0$	1	−1	0	0	2	0	0

Table 11. Values of SU(4) invariants for ground state ($1/2^+ \to 3/2^+ +$ meson) transitions. Further explanation as in caption of Table 10

	I_1^*	I_2^*		I_1^*	I_2^*
$6\,\Lambda_c^+ \to \Sigma^{*0}\pi^+$	0	2	$6\,\Xi_c^0 \to \Sigma^{*0}\bar{K}^0$	0	−2
$6\,\Lambda_c^+ \to \Sigma^{*+}\pi^0$	0	2	$\sqrt{18}\,\Xi_c^0 \to \Sigma^{*+}K^-$	0	−2
$\sqrt{108}\,\Lambda_c^+ \to \Sigma^{*+}\eta_8$	0	6	$6\,\Xi_c^0 \to \Xi^{*0}\pi^0$	0	−2
$\sqrt{54}\,\Lambda_c^+ \to \Sigma^{*+}\eta_1$	0	0	$\sqrt{108}\,\Xi_c^0 \to \Xi^{*0}\eta_8$	0	2
$\sqrt{18}\,\Lambda_c^+ \to \Delta^+\bar{K}^0$	0	−2	$\sqrt{54}\,\Xi_c^0 \to \Xi^{*0}\eta_1$	0	−4
$\sqrt{6}\,\Lambda_c^+ \to \Delta^{++}K^-$	0	−2	$\sqrt{18}\,\Xi_c^0 \to \Xi^{*-}\pi^+$	0	2
$\sqrt{18}\,\Lambda_c^+ \to \Xi^{*0}K^+$	0	2	$\sqrt{6}\,\Xi_c^0 \to \Omega^-K^+$	0	2
$\sqrt{18}\,\Xi_c^+ \to \Sigma^{*+}\bar{K}^0$	0	0	$\sqrt{3}\,\Omega_c^0 \to \Xi^{*0}\bar{K}^0$	−1	0
$\sqrt{18}\,\Xi_c^+ \to \Xi^{*0}\pi^+$	0	0	$\Omega_c^0 \to \Omega^-\pi^+$	−1	0

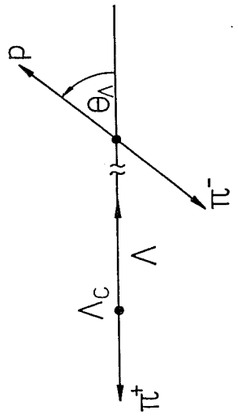

Fig.2

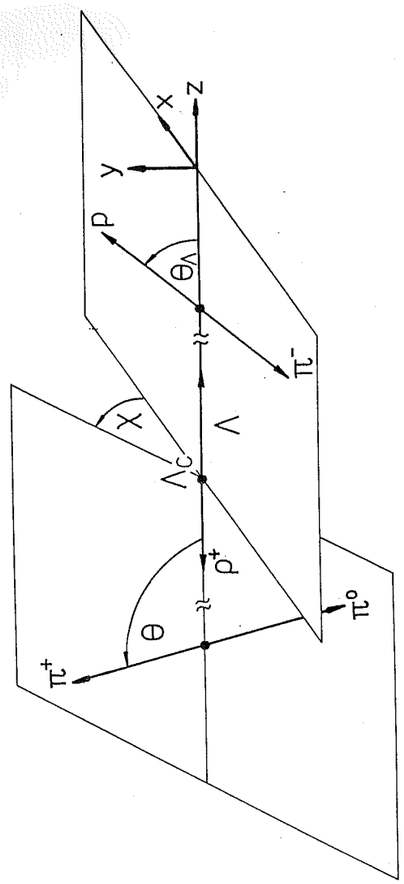

Fig.3

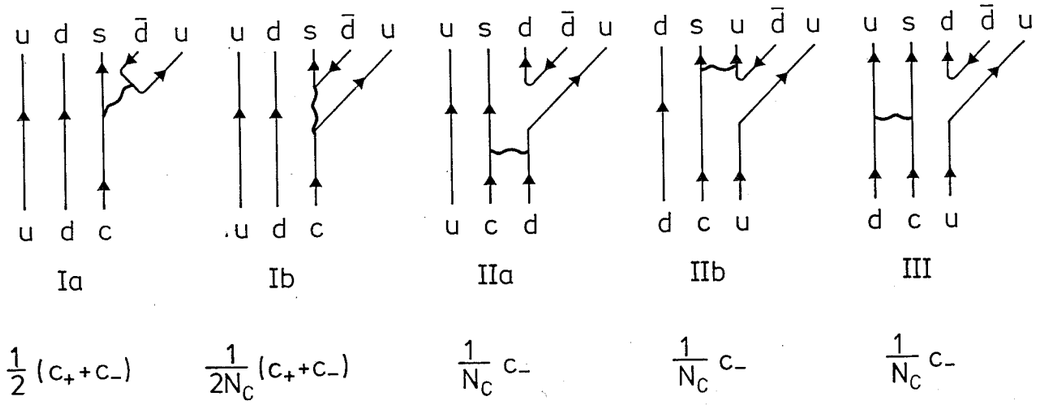

Fig.1